

## 喷昔洛韦-铜(II)配合物的合成、晶体结构及 DNA 键合作用

刘瑞雪<sup>1</sup> 赖德霖<sup>1</sup> 邓前军<sup>\*2</sup> 程凤杰<sup>1</sup> 范兰琼<sup>1</sup> 刘延成<sup>\*,1</sup>

(<sup>1</sup> 广西师范大学化学与药学学院, 省部共建药用资源化学与药物分子工程国家重点实验室, 桂林 541004)

(<sup>2</sup> 佛山科学技术学院材料科学与能源工程学院, 佛山 528000)

**摘要:** 将具有生物活性的铜(II)离子与临床抗病毒药物喷昔洛韦(PCV)配位, 合成了首个喷昔洛韦的金属配合物 $[\text{Cu}(\text{PCV})_2(\text{H}_2\text{O})_3]\text{SO}_4$  (**1**), 并通过红外光谱、元素分析和 X 射线单晶衍射分析方法对其结构进行了表征。初步测试了其针对多种典型人肿瘤细胞株的体外抗肿瘤活性。测试结果表明, 喷昔洛韦-铜(II)配合物 **1** 对各种肿瘤细胞株均显示出显著高于喷昔洛韦的增殖抑制活性, 其中对于较为敏感的人肝癌细胞 BEL-7404, 配合物 **1** 的增殖抑制活性是喷昔洛韦的 3 倍以上。进一步, 针对抗肿瘤首要靶点 DNA, 通过紫外-可见吸收光谱、荧光发射光谱以及 DNA 粘度实验对配合物 **1** 与小牛胸腺 DNA 的键合作用方式进行了探讨。由实验结果推测, DNA 应该是配合物 **1** 的抗肿瘤活性的重要靶点, 其与 DNA 之间存在典型的插入结合方式。

**关键词:** 喷昔洛韦; 金属配合物; 铜(II); 抗肿瘤活性; DNA 键合

中图分类号: O614.121

文献标识码: A

文章编号: 1001-4861(2019)01-0125-08

DOI: 10.11862/CJIC.2019.013

## Synthesis, Crystal Structure and DNA Binding of Copper(II) Complex of Penciclovir

LIU Rui-Xue<sup>1</sup> LAI De-Lin<sup>1</sup> DENG Qian-Jun<sup>\*2</sup> CHENG Feng-Jie<sup>1</sup> FAN Lan-Qiong<sup>1</sup> LIU Yan-Cheng<sup>\*,1</sup>

(<sup>1</sup>School of Chemistry and Pharmaceutical Sciences, State Key Laboratory for the Chemistry and Molecular Engineering of Medicinal Resources, Guangxi Normal University, Guilin, Guangxi 541004, China)

(<sup>2</sup>School of Material Science and Energy Engineering, Foshan University, Foshan, Guangdong 528000, China)

**Abstract:** The first metal complex of the clinical antiviral agent, penciclovir (PCV), was synthesized and structurally characterized by IR, elemental analysis and X-ray single crystal diffraction analysis. In this complex, copper(II) was selected as the bioactive metal center, which was coordinated by two PCV molecules to form a new copper(II) complex of PCV,  $[\text{Cu}(\text{PCV})_2(\text{H}_2\text{O})_3]\text{SO}_4$  (**1**). The *in vitro* antitumor activity of complex **1** towards a variety of typical human tumor cell lines has been explored. The results indicated that complex **1** showed enhanced antitumor activity comparing with PCV alone towards all the tested cell lines, in which the human hepatoma cell line BEL-7404 was the most sensitive one to complex **1** (Inhibition ratio  $(55.83 \pm 16.41)\%$ ). The inhibitory activity of complex **1** is more than 3 times that of PCV (Inhibition ratio  $(17.38 \pm 5.53)\%$ ). Furthermore, the DNA binding mechanism of complex **1** was also studied and discussed by means of UV-Vis absorption and fluorescence emission spectral analyses, as well as the DNA viscosity experiment. The results suggested that DNA, as the primary antitumor target, should be an important binding target of complex **1**. And the classic intercalative binding mode might exist between complex **1** and CT-DNA. CCDC: 1825089.

**Keywords:** penciclovir; metal complex; copper(II); antitumor activity; DNA binding

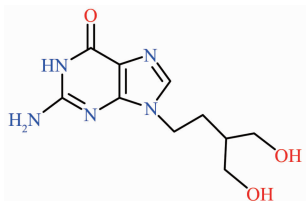
收稿日期: 2018-06-13。收修改稿日期: 2018-10-29。

国家自然科学基金(No.21561005), 广西自然科学基金(No.2017GXNSFDA198048), 广东省材料科学重点学科开放基金资助项目(No.2017-13)和广西医药产业人才小高地项目(No.1405/1505)资助

\*通信联系人。E-mail: yeliu@gxnu.edu.cn, 1192097240@qq.com

## 0 Introduction

Nucleoside drugs are a series of therapeutic agents for viral diseases. In particular, the successful development of the antiviral drug, acyclovir, marked the opening of a new era for anti-herpes virus drugs<sup>[1]</sup>. Nucleoside drugs are classified into the following categories: antiretroviral drugs, anti-herpes virus drugs, anti-cytomegalovirus drugs and so on<sup>[2-3]</sup>. As the acyclovir derivative, penciclovir (PCV) is one of the most successful nucleoside drugs<sup>[4-6]</sup>, which is developed by SmithKline Beecham of U.S. It is the metabolic product of the precursor drug of acyclovir actually, and it can inhibit the proliferation of the herpes simplex virus, herpes zoster and EB virus effectively<sup>[5,7]</sup>. Its action mechanism is similar to acyclovir, but with the increased cell accumulation and survival rate, which can maintain the antiviral activity effectively. Meanwhile, the side effects are reduced obviously. PCV can also block the normal band-lymphocyte lesions caused by EB virus. Therefore, it can be assumed that PCV not only exhibits a significant effect on the herpes virus<sup>[8-10]</sup>, but also shows certain resistance to the lymphatic cancer.



Scheme 1 Chemical structure of PCV

Cancer has endangered the health of human beings seriously since the 20th century. It is generally accepted that cancer is caused by the disorder of cell growth and proliferation mechanisms<sup>[11]</sup>. Most of the antitumor drugs were primarily exert their antitumor mechanisms by preventing the synthesis of DNA, RNA and protein, or by acting on these large molecules directly<sup>[12]</sup>. Therefore, nucleotide drugs can be considered potential anticancer drugs, although they are not yet fully applied to the cancer treatment.

On the other hand, the discovery of cisplatin as new metal-based anticancer drug and its clinical application have explored a new and broad field of

anticancer drugs development<sup>[13-15]</sup>. More and more metal complexes have been synthesized and designed in recent years. As an indispensable element of human body, copper(II) has attracted an increasing number of researchers to explore its potential biological applications from its metal complexes, especially for its potential anticancer activity, since quite some copper(II) complexes were found to be significantly higher cytotoxic against some human tumor cell lines<sup>[16-18]</sup>. Herein we selected PCV as a typical nucleotide drug targeting DNA, and combined it with copper(II) by coordination chemistry method, to obtain the first metal complex of PCV,  $[\text{Cu}(\text{PCV})_2(\text{H}_2\text{O})_3]\text{SO}_4$  (**1**). This new complex **1** was structurally characterized and was screened on its *in vitro* antitumor activity. Its DNA binding property with CT-DNA was also discussed by means of typical experimental methods.

## 1 Experimental

All the starting materials and the reaction solvents were commercial available with reagent grade and were used without further purification. PCV was purchased from Yuancheng Co. Ltd. of Hubei Province.  $\text{CuSO}_4 \cdot 5\text{H}_2\text{O}$  and the reaction solvents were all purchased from Xilong Co. Ltd. of Guangdong Province. Calf thymus DNA (CT-DNA), MTT, Tris and PBS were all purchased from Sigma-Aldrich.

### 1.1 Synthesis of complex 1

Penciclovir (PCV) (0.2 mmol, 0.050 6 g) and  $\text{CuSO}_4 \cdot 5\text{H}_2\text{O}$  (0.15 mmol, 0.037 5 g) were put into a Pyrex glass tube, adding to 1 mL of mixed solvent of ethanol and water (3:1, V/V). The reaction mixture was frozen by liquid  $\text{N}_2$ , and then the tube was vacuumed and sealed by a torch. Then it was placed in 80 °C in the dark for 48 h, before it was gradually cooled down to room temperature. The green crystals were harvested, which were determined to be the title complex **1** (Yield: 66%). The green stick crystals suitable for X-ray single crystal diffraction analysis was selected to determine the structure. IR (KBr,  $\text{cm}^{-1}$ ): 3 400, 2 931, 2 375, 1 666, 1 633, 1 487, 1 413, 1 384, 1 120, 1 033, 859, 776, 689, 619, 510. Anal. Calcd. for  $\text{C}_{20}\text{H}_{42}\text{CuN}_{10}\text{O}_{16}\text{S}$ (%): C, 31.00; H, 5.42; N, 18.08. Found(%): C

29.77, H 5.68, N 17.93.

## 1.2 X-ray structure analysis

The data collection of single crystal was carried out on a Rigaku Mercury CCD equipped with a graphite monochromated Mo  $K\alpha$  radiation ( $\lambda=0.071\ 073\ \text{nm}$ ). The structures were solved with direct methods and refined using SHELX-97<sup>[19]</sup> programs. The non-hydrogen atoms were located in successive difference Fourier synthesis. The final refinement was performed by full-

matrix least-squares methods with anisotropic thermal parameters for non-hydrogen atoms on  $F^2$ . The hydrogen atoms were added theoretically and riding on the concerned atoms. No H atoms associated with guest water molecules were located from the difference Fourier map. The crystallographic data and refinement details of the structure analyses were summarized in Table 1 and Table 2.

CCDC: 1825089.

**Table 1 Crystal data and structural refinement parameters for complex 1**

Empirical formula	$\text{C}_{20}\text{H}_{12}\text{CuN}_{10}\text{O}_{16}\text{S}$	$\mu / \text{mm}^{-1}$	6.284
Formula weight	774.26	$F(000)$	12 750
Temperature / K	293(2)	Crystal size / mm	0.40×0.23×0.15
Crystal system	Monoclinic	$2\theta$ range for data collection / (°)	6.18–50
Space group	$P2_1/n$	Index range	$-15 \leq h \leq 15, -16 \leq k \leq 16, -21 \leq l \leq 20$
$a / \text{nm}$	1.270 2(3)	Reflection collected	18 102
$b / \text{nm}$	1.420 7(3)	Independent reflection	5 643 ( $R_{\text{int}}=0.083\ 2$ )
$c / \text{nm}$	1.786 2(4)	Data, restraint, parameter	5 643, 96, 455
$\beta / (^\circ)$	90.18(3)	Goodness-of-fit on $F^2$	1.062
Volume / $\text{nm}^3$	3.223 3(11)	Final $R$ index [ $I \geq 2\sigma(I)$ ]	$R_1=0.111\ 2, wR_2=0.266\ 1$
$Z$	30	Final $R$ index (all data)	$R_1=0.148\ 3, wR_2=0.288\ 5$
$D_c / (\text{g}\cdot\text{cm}^{-3})$	12.523	Largest diff. peak and hole / ( $\text{e}\cdot\text{nm}^{-3}$ )	209 and $-760$

**Table 2 Selected bond lengths (nm) and bond angles (°) for complex 1**

Cu1-N1	0.197 6(7)	Cu1-O9	0.201 1(6)	C6-N6	0.139 4(11)
Cu1-N6	0.198 7(7)	C2-N6	0.130 7(12)	C1-C6	0.140 8(12)
Cu1-O7	0.198 9(7)	C5-N1	0.137 6(10)		
Cu1-O8	0.216 2(6)	C9-N1	0.146 8(9)		
N1-Cu1-N6	170.8(3)	N6-Cu1-O7	89.6(3)	O7-Cu1-O9	160.2(3)
N1-Cu1-O7	87.6(3)	N6-Cu1-O8	98.9(3)	O9-Cu1-O8	103.5(3)
N1-Cu1-O8	90.2(3)	N6-Cu1-O9	88.0(3)		
N1-Cu1-O9	91.6(3)	O7-Cu1-O8	96.3(3)		

## 1.3 In vitro cytotoxicity

The human tumor cell lines, including BEL-7404, SGC-7901, HeLa, MCF-7 and A549, were obtained from the Shanghai Cell Bank of Chinese Academy of Science.

The title complex, complex **1**, compared with PCV as positive control, were dissolved in DMSO to prepare the  $5.00\ \text{mmol}\cdot\text{L}^{-1}$  DMSO stock solutions. Each cell was maintained with the medium supplemented containing the fetal bovine and other essential medium in order to guarantee a good state of

survival before it was tested. Then they were transferred to 96-well plants as far as possible to ensure the number of cells in each well plant was similar. After 24 h of continuous culturing in the  $37\ ^\circ\text{C}$  incubator, cells growth reached 70% in the well. Then each compound was added to the wells, which has been diluted with the phosphate buffer saline (PBS) solution already, and then proceeded to culture for 48 h in 5% (V/V)  $\text{CO}_2$  humidified atmosphere. After 48 h of cultivation, 0.1 mg of MTT (dissolved in 20  $\mu\text{L}$  PBS) was added to each well. Finally, the formed

blue formazan crystals were dissolved in 100  $\mu\text{L}$  of DMSO, and the absorbance was measured using the enzyme-labeled reading instrument with 490 nm/630 nm double wavelength. The growth inhibition ratio for each cell line under the concentration of 20  $\mu\text{mol}\cdot\text{L}^{-1}$  of complex **1** or PCV was evaluated according to the absorbance, ultimately.

#### 1.4 UV-Vis absorption and fluorescence spectral analysis

Tris-NaCl buffer solution (which included 5 mmol Tris, 50 mmol NaCl, and was adjusted to pH=7.3 by hydrochloric acid) was prepared using double distilled water. The 5.00  $\text{mmol}\cdot\text{L}^{-1}$  DMSO stock solution of complex **1** was used for DNA binding studies. It was diluted by Tris buffer to prepare the corresponding working solutions with the concentration of 20  $\mu\text{mol}\cdot\text{L}^{-1}$ , in which the final DMSO concentration was no more than 1%. CT-DNA was also dissolved in Tris buffer solution to give a final concentration of 2.00  $\text{mmol}\cdot\text{L}^{-1}$ , and it was kept at 4  $^{\circ}\text{C}$  for no more than 5 days before using.

The UV-Vis absorption spectroscopy was a kind of classic technique to study the interaction between small molecules and DNA. The absorbance of each sample was recorded on a PerkinElmer Lambda45 UV-Visible Spectrophotometer, in the wavelength range from 200 to 700 nm. The fluorescence spectra were recorded on a Shimadzu RF-5301/PC spectrofluorophotometer, in the wavelength range from 350 to 700 nm, with slit width of 15 nm. The optimized excited wavelength ( $\lambda_{\text{ex}}$ ) of the fluorescence emission

was determined to be 340 nm.

#### 1.5 DNA viscosity experiment

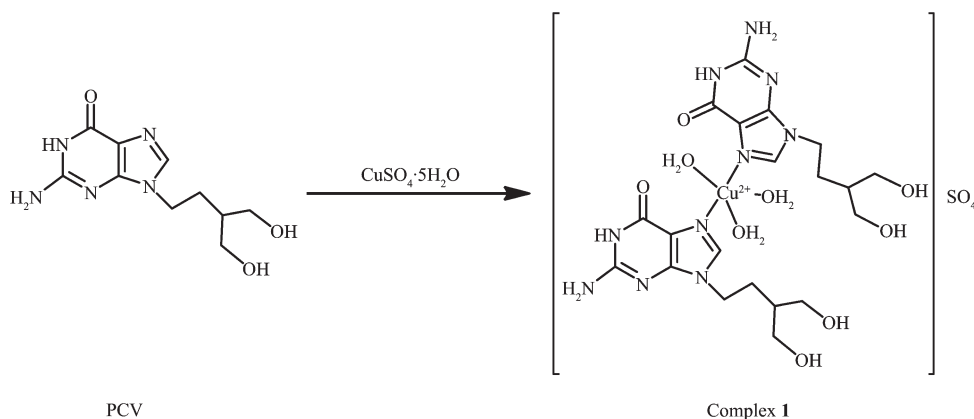
DNA viscosity experiment was recorded on a Brookfield DV-II pro digital viscometer equipped with TC-502D thermostatic bath. A 20 mL of CT-DNA solution ( $1.80\text{ mmol}\cdot\text{L}^{-1}$ ) was prepared in Tris buffer as a working solution for DNA viscosity experiment. The stock solution of complex **1** was added according to the gradual increasing ratios for  $c_1/c_{\text{DNA}}$  from 0.01 to 0.09. The circulating bath temperature was maintained at  $(35.0\pm0.5)^{\circ}\text{C}$ . The viscosity value,  $\eta$  ( $\text{mPa}\cdot\text{s}$ ), was obtained by running the spindle in working samples at  $30\text{ r}\cdot\text{min}^{-1}$  via the equipped ULA adapter. The data were presented directly as plot of  $\eta$  versus  $c_1$ . The effect of DMSO on the viscosity was eliminated based on its 100% viscosity value of  $2.03\text{ mPa}\cdot\text{s}$  measured at  $35.0^{\circ}\text{C}$ .

## 2 Results and discussion

### 2.1 Synthesis and structural characterization of complex **1**

As shown in Scheme 2, the synthetic reaction for the title complex, complex **1**, has been stated in the experimental section. The product yielded green crystals. The complex was characterized by IR, elemental analysis, and its coordination geometry was determined by X-ray single crystal diffraction analysis.

As shown in Fig.1, the crystal structure of complex **1** shows a distorted trigonal bipyramid coordination mode, in which two PCV ligands coordinate to the central Cu(II) via the N atom of



Scheme 2 Synthetic route of complex **1**

imidazole, and occupied the axial positions of the bipyramid, respectively. Three  $\text{H}_2\text{O}$  molecules occupy the equatorial plane of the trigonal bipyramid via the coordinated O atoms. The Cu-N bond lengths are 0.197 6(7) nm (Cu1-N1) and 0.198 7(7) nm (Cu1-N6), respectively, while the angle of N1-Cu1-N6 is  $170.8(3)^\circ$ . The Cu-O bond lengths are 0.198 9(7) nm (Cu1-O7), 0.216 2(6) nm (Cu1-O8) and 0.201 1(6) nm (Cu1-O9), respectively. Each coordinating unit showed +2 positive charged, and one sulfate anion ( $\text{SO}_4^{2-}$ ) existed in each unit as the counter-ion.

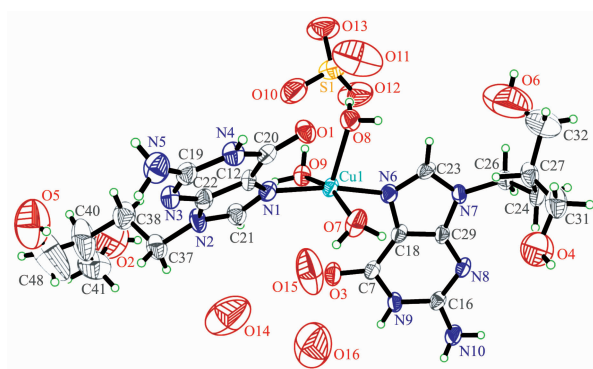


Fig.1 ORTEP presentation of the crystal structure of complex **1** in a 50% ellipsoid

## 2.2 *In vitro* cytotoxicity screening

The *in vitro* cytotoxicity was tested as a preliminary screening by MTT assay, towards a series of tumor cell lines, including the A549, BEL-7404, SGC-7901, HeLa and MCF-7. The screening concentration for complex **1**, PCV and  $\text{CuSO}_4 \cdot 5\text{H}_2\text{O}$  was equal to 20

$\mu\text{mol} \cdot \text{L}^{-1}$ . The results were listed in Table 3.

Viewed from the data of the screening test, complex **1** showed higher growth inhibition abilities than PCV alone in terms of all these tested tumor cell lines. The inhibition ratio of PCV did not exceed 50% under  $20 \mu\text{mol} \cdot \text{L}^{-1}$ . Comparatively, the inhibition ratios for complex **1** toward all the tumor cell lines were higher than 50%. The growth inhibition ratios of complex **1** were higher than PCV in the range from *ca.* 20% to 220%. Especially, the growth inhibition ratios for complex **1** against BEL-7404 and A549 were about 2 and 3 times of those for PCV, respectively. Furthermore,  $\text{CuSO}_4 \cdot 5\text{H}_2\text{O}$  as the raw metal salt was found to cytotoxic selectively on the BEL-7404 and SGC-7901 tumor cell lines. However, it is much less cytotoxic against the other three tumor cell lines. It should be noticed that  $\text{CuSO}_4$  alone can't function as an effective antitumor agent. So PCV might be also regarded as an appropriate carrier to bring Cu(II) into the cells to exert its bioactivity. In all, it suggested that there is the positive synergistic effect when combining the PCV and Cu(II) towards some typical tumor cell lines, such as HeLa, MCF-7 and A549. The enhancement on the antitumor activity of complex **1** might be ascribed to the combination of PCV and Cu(II), where the central Cu(II) plays a key role<sup>[16-18]</sup>. This is of positive significance for exploring new applications on PCV as new type of drugs.

Table 3 Cell growth inhibition ratios induced by PCV, complex **1** and  $\text{CuSO}_4 \cdot 5\text{H}_2\text{O}$  towards five typical human tumor cell lines

Compound	%		
	PCV	Complex <b>1</b>	$\text{CuSO}_4 \cdot 5\text{H}_2\text{O}$
BEL-7404	17.38±5.53	55.83±16.41	64.39±2.77
SGC-7901	40.32±6.00	51.90±6.57	61.95±7.90
HeLa	47.74±8.96	56.94±4.03	24.24±0.25
MCF-7	35.34±3.01	50.03±2.84	41.26±5.95
A549	31.65±1.75	62.40±3.87	35.33±0.15

## 2.3 DNA binding analysis

DNA is widely recognized as a target for many antitumor drugs. The mechanism of interaction between small molecules and DNA has been studied for several decades, so not only it is necessary to

study the DNA binding mechanism of new compounds, but also the study has important significance for designing DNA-targeting drugs. Therefore, the DNA binding property of complex **1** was studied by UV-Vis, fluorescence spectroscopy,



and DNA viscosity experiment, which are the most classic methods for the DNA binding study.

### 2.3.1 UV-Vis absorption analysis

The UV-Vis absorption spectral analysis was firstly applied to study the DNA binding property of the complex. As shown in Fig.2, the UV-Vis spectrum of complex **1** in the absence of CT-DNA (dashed line) showed the maximum absorption peak at 252 nm, which corresponds to the  $\pi \rightarrow \pi^*$  electronic transition of **1**. With the increasing amounts of CT-DNA, it was found that the maximum absorbance at 252 nm decreased by gradient (solid lines). When the DNA concentration reached  $1.6 \times 10^{-4} \text{ mol} \cdot \text{L}^{-1}$ , the maximum absorbance ( $A_{\text{max}}$ ) of complex **1** decreased from 0.422 to 0.369, with a decreasing ratio of 12.6%. It suggested an intercalative binding mode for complex **1** to DNA, since the small molecules intercalated between the neighboring base pairs of DNA might weaken the  $\pi \rightarrow \pi^*$  electronic transition and lead to obvious hypochromic effect. However, comparing with the binding constant of EtBr, which is the classic DNA intercalator, the intercalative binding ability of complex **1** to DNA might be not strong.

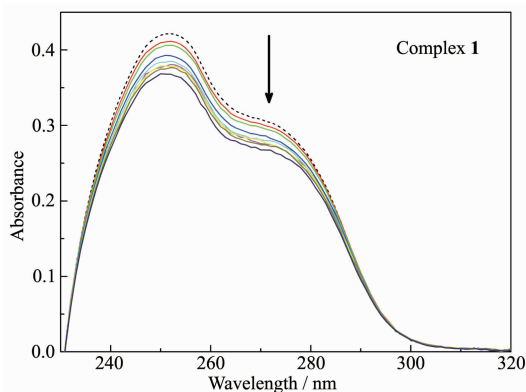


Fig.2 UV-Vis absorption spectra of complex **1** in the absence (dashed line) and presence (solid lines) of CT-DNA with increasing concentration ratios ( $c_{\text{DNA}}/c_1$ ) in the range from 1:1 to 8:1

### 2.3.2 Fluorescence spectra analysis

Fluorescence quenching is a phenomenon of the reduction on the fluorescence intensity caused by the interaction between the fluorescent molecules and the quenching molecules. In water solution, the fluorescent molecules may be quenched by  $\text{H}_2\text{O}$

molecules. But when they intercalated between the neighboring base pairs of DNA, they might be protected by the hydrophobic circumstance of DNA, so that their fluorescence would not be quenched.

As shown in Fig.3, in the absence of CT-DNA, the fluorescence emitted of complex **1** at  $20 \mu\text{mol} \cdot \text{L}^{-1}$  was very weak. The maximum fluorescent emission peak was at 470 nm, with fluorescence intensity of  $I = 45.4$ , as indicated by the dashed line. After the addition of increasing amounts of CT-DNA, it was found that the fluorescence intensity of complex **1** enhanced obviously. The fluorescence intensity enhanced to  $I = 136.52$  when the  $c_{\text{DNA}}/c_1 = 1:1$ , which was *ca.* 3 times of complex **1** alone. When the concentration of DNA reached  $1.4 \times 10^{-4} \text{ mol} \cdot \text{L}^{-1}$ , with  $c_{\text{DNA}}/c_1 = 7:1$ , the fluorescent intensity of complex **1** enhanced to 487.3, which was more than 10 times of complex **1** alone. And then the fluorescent intensity of this complex tended to be saturated with further addition of DNA. It further suggested that complex **1** might bind DNA by an intercalative mode, so that its fluorescent emission was effectively prevented from quenching by  $\text{H}_2\text{O}$ . Herein, we assumed that the central Cu(II) played a key role in facilitating the DNA binding ability of PCV.

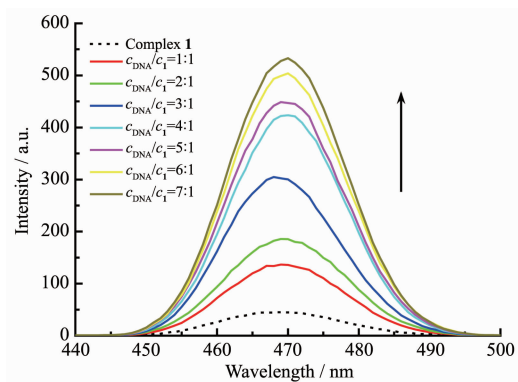


Fig.3 Fluorescent emission spectra of complex **1** in the absence and presence of CT-DNA with increasing concentration ratios ( $c_{\text{DNA}}/c_1$ ) in the range from 1:1 to 7:1

### 2.3.3 DNA viscosity experiment

When the small molecules intercalated between the neighboring base pairs of DNA, the viscosity of the DNA solution will increased due to the lengthening of the DNA double helix. So the DNA

viscosity experiment was generally considered to be a more direct method to determine the DNA binding mode of small molecules, which might be possible to further confirm the interaction mechanism of complex **1** with DNA.

As shown in Fig.4, the viscosity of the DNA solution alone was measured to be  $\eta_0=3.495 \text{ mPa}\cdot\text{s}$ , when the rotational speed was  $50 \text{ r}\cdot\text{min}^{-1}$  and the temperature of solution was  $30\text{ }^\circ\text{C}$ . However, with the increasing amounts of complex **1** added, the viscosity of the DNA solution increased significantly. When the ratio of  $c_1/c_{\text{DNA}}$  reached 0.09, the viscosity increased to  $\eta=3.660 \text{ mPa}\cdot\text{s}$ , with  $\eta/\eta_0=1.05$ . So it also suggested that complex **1** should bind with CT-DNA via a classic intercalative mode, resulting in the significant enhancement on the viscosity of the DNA solution.

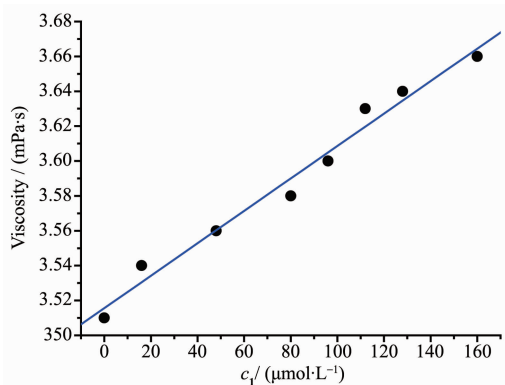


Fig.4 Viscosity measurement of CT-DNA solution under the addition of increasing concentrations of complex **1**, with the ratios of  $c_1/c_{\text{DNA}}$  in the range from 0.02 to 0.09

### 3 Conclusions

In this work, a new copper(II) complex of the antiviral drug, penciclovir(PCV), was synthesized and structurally characterized. To our knowledge, this is the first metal complex of penciclovir reported. Further, its in vitro antitumor activity was screened, which indicated that the antitumor activity towards several typical tumor cell lines was significantly improved when PCV coordinated with Cu(II). Subsequent studies strongly suggested that the complex could bind with CT-DNA via an intercalative binding mode, even though it was not as strong as the classic DNA intercalator, EtBr. This was supported by

the experimental results, including the hypochromicity from the UV-Vis spectra and the increase on the fluorescence intensity of the complex under the addition of CT-DNA, as well as the enhancement on the viscosity of the DNA solution when bound with the complex. It suggested that the Cu(II) played an indispensable role in the complex. In addition, considering the bioactivity of Cu(II) itself, it provided an approach for designing and developing new type of drugs from penciclovir. And the further studies on its antiviral activity towards HSV might help to explore new metal-based antiviral drugs.

**Acknowledgements:** This work was supported by the National Natural Science Foundation (Grant No.21561005), the Natural Science Foundation of Guangxi Province (Grant No. 2017GXNSFDA198048), the Open Foundation of Characteristic Key Subject on Materials of Guangdong Province (Grant No. 2017-13) and the Talents' Small Highland in Medicinal Industry of Guangxi (Grant No.1405/1505).

### References:

- [1] Parker W B. *Chem. Rev.*, **2009**,**109**:2880-2893
- [2] Schaeffer H J, Beauchamp L, de Miranda P, et al. *Nature*, **1978**,**272**:583-585
- [3] Sime J T, Barnes R D, Elson S W, et al. *J. Chem. Soc. Perkin Trans.*, **1992**,**1**:1653-1658
- [4] Elion G B, Furman P A, Fyfe J A, et al. *Proc. Natl. Acad. Sci. USA*, **1977**,**74**:5716-5720
- [5] Kim H O, Baek H W, Moon H R, et al. *Org. Biomol. Chem.*, **2004**,**2**:1164-1168
- [6] Freeman S, Gardiner J M. *Mol. Biotechnol.*, **1996**,**5**:125-137
- [7] TAN Zai-You(谭载友), JIANG Tao(江涛), TANG Chun-Ping(唐春萍), et al. *Chinese Journal of New Drugs(中国新药杂志)*, **2003**,**12**(7):529-531
- [8] Zhong M G, Xiang Y F, Qiu X X, et al. *RSC Adv.*, **2013**,**3**: 313-328
- [9] Siakallis G, Spandidos D A, Sourvinos G. *Antiviral Ther.*, **2009**,**14**:1051-1064
- [10] Greco A, Diaz J J, Thouvenot D, et al. *Infect. Disord.: Drug Targets*, **2007**,**7**:11-18
- [11] Brem S. *Cancer Control*, **1999**,**6**:436-458
- [12] Yang D Z, Wang A H J. *Prog. Biophys. Molec. Biol.*, **1996**, **66**:81-111
- [13] Takahara P M, Rosenzweig A C, Frederick C A. *Nature*, **1995**,**377**:649-652

- [14]Takahara P M, Frederick C A, Lippard S J. *J. Am. Chem. Soc.*, **1996**,**118**:12309-12321
- [15]Reedijk J. *Chem. Commun.*, **1996**:801-806
- [16]HAI Shi-Kun(海士坤), LOU Shu-Fang(娄淑芳), QIU Xiao-Yang(仇晓阳). *Chinese J. Inorg. Chem.*(无机化学学报), **2016**,**32**:906-912
- [17]HAN Xue-Feng(韩学锋), CAI Hong-Xin(蔡红新), JIA Lei (贾磊), et al. *Chinese J. Inorg. Chem.*(无机化学学报), **2015**, **31**:1453-1459
- [18]Lewis A, McDonald M, Scharbach S, et al. *J. Inorg. Biochem.*, **2016**,**157**:52-61
- [19]Sheldrick G M. *SHELX-97, Program for the Solution and the Refinement of Crystal Structures*, University of Göttingen, Germany, **1997**.